agriculture

MDPI

Article

Numerical Analysis of Ventilation Efficiency of a Korean Venlo-Type Greenhouse with Continuous Roof Vents

Se-Jun Park [1], In-Bok Lee [2,3,*], Sang-Yeon Lee [1], Jun-Gyu Kim [1], Young-Bae Choi [1], Cristina Decano-Valentin [1,4], Jeong-Hwa Cho [1], Hyo-Hyeog Jeong [1] and Uk-Hyeon Yeo [5]

1 Department of Rural Systems Engineering, Research Institute for Agriculture and Life Sciences, College of Agriculture and Life Sciences, Seoul National University, 1, Gwanakno, Gwanak-gu, Seoul 08826, Korea
2 Department of Rural Systems Engineering, Research Institute for Agriculture and Life Sciences, Global Smart Farm Convergence Major, College of Agriculture and Life Sciences, Seoul National University, 1, Gwanakno, Gwanak-gu, Seoul 08826, Korea
3 Research Institute of Green Eco Engineering, Institute of Green Bio Science and Technology, Seoul National University, 1477, Pyeongchang-daero, Daehwa-myeon, Pyeongchang-gun 25354, Korea
4 Department of Agricultural and Biosystems Engineering, College of Engineering, Mariano Marcos State University, Batac 2906, Philippines
5 Agriculture, Animal & Aquaculture Intelligence Research Center, Electronics and Telecommunications Research Institute, 218 Gajeong-ro, Yuseong-gu, Daejeon 34129, Korea
* Correspondence: iblee@snu.ac.kr; Tel.: +82-2-880-4586; Fax: +82-2-873-2087

check for updates

Citation: Park, S.-J.; Lee, I.-B.; Lee, S.-Y.; Kim, J.-G.; Choi, Y.-B.; Decano-Valentin, C.; Cho, J.-H.; Jeong, H.-H.; Yeo, U.-H. Numerical Analysis of Ventilation Efficiency of a Korean Venlo-Type Greenhouse with Continuous Roof Vents. *Agriculture* **2022**, *12*, 1349. https://doi.org/10.3390/agriculture12091349

Academic Editors: Muhammad Sultan, Redmond R. Shamshiri, Md Shamim Ahamed and Muhammad Farooq

Received: 30 June 2022
Accepted: 19 August 2022
Published: 31 August 2022

Publisher's Note: MDPI stays neutral with regard to jurisdictional claims in published maps and institutional affiliations.

Abstract: A Venlo-type greenhouse with a continuous roof vent (CR-Venlo greenhouse) was proposed by the Ministry of Agriculture, Food and Rural Affairs, South Korea (2019) for natural ventilation even during summers. It is ventilated through the buoyancy effect of the heated air using the high eave elevation. However, the CR-Venlo greenhouse was not distributed domestically, and its ventilation efficiency was not quantitatively evaluated. We aimed to analyze the natural ventilation efficiency of the greenhouse according to the eave height, using computational-fluid-dynamics. The simulation model was analyzed for hot summer conditions. The target greenhouse is ventilated only through the roof vent with all roof windows open; therefore, the air introduced through the roof window is easily exhausted. To evaluate the efficiency of ventilation, the external air entering through the roof window was calculated and evaluated. The amount of incoming air varied greatly with the location of the span and average temperature of the greenhouse; The temperature of the crop zone decreased lognormally with increasing height of the eave. Moreover, the ventilation efficiency of CR-Venlo greenhouse could be increased by improving the ventilation structure such as a shape, position or combination of roof window.

Keywords: computational fluid dynamics (CFD); eave height; natural ventilation; venlo greenhouse

1. Introduction

Crop production through facility cultivation has developed continuously over the past several years by ensuring stable productivity and high-quality crops throughout the year. Recent data from the Ministry of Agriculture, Food and Rural Affairs, South Korea (MAFRA) indicated that the scale of production has been steadily increasing from the 1970s to the present; the area of domestic vegetable cultivation and total production were 54,443 ha and 2,441,000 tons in 2019, respectively [1]. Meanwhile, the domestic agricultural population is steadily aging and declining, whereas the demand for agricultural products has been growing. In addition, there is an increase in automation and the number of large-scale greenhouses. The development of ICT technology and the expansion of investments in smart farms are accelerating the enlargement of greenhouses. In particular, the area of multi-span greenhouses in Korea increased from 5227 ha in 2012 to 7088 ha in 2019 [1]. A large greenhouse enables easy automation and improved productivity. It has the advantage of

relatively low heating cost in winter but, inevitably, the disadvantage of having a large cooling demand in high-temperature environments in summer.

Therefore, a Venlo-type greenhouse with a continuous roof vent (CR-Venlo greenhouse) has been developed by the MAFRA in 2019 to reduce high-temperature stress to crops even in high-temperature environments in summer. The CR-Venlo greenhouse has a structure similar to that of the conventional Venlo-type greenhouse (C-Venlo greenhouse). Ventilation occurs due to the buoyancy effect of heated air inside the greenhouse in summer due to the high eave height. Most of the roof area of the CR-Venlo greenhouse is designed with roof vents; therefore, there is the possibility of wind ventilation using a large roof vent. In particular, the temperature inside the greenhouse decreases as the elevation of the eave increases [1]; therefore, the temperature difference between the inside and outside of the greenhouse decreases. In this study, we evaluated a single-span greenhouse and designed the opening angle of the roof window to be significantly large. In a single-span greenhouse, the natural ventilation effect is greater than that in a multi-span greenhouse. When the opening angle of the roof window is considerably large, the inflow of external air into the greenhouse is smooth. Furthermore, in a single-span greenhouse, the influence of side window ventilation is great. However, in a multi-span greenhouse, the ventilation effect by the side windows decreases rapidly as the number of the multi-span increases. Therefore, the ventilation through the roof window is highly important for the stagnant area of the multi-span greenhouse. The roof vent window should be designed based on the quantitative analysis of natural ventilation. The CR-Venlo greenhouse has a high ventilation efficiency due to the structural characteristics of the ventilation window; however, its ventilation efficiency has not yet been quantitatively evaluated [2].

Changes in the thermal environment inside the greenhouse according to ventilation design have been well studied [3–18]. Most studies analyze the horizontal temperature distribution at a specific height, such as the height of a crop. Only a few studies have been reported on the vertical temperature distribution inside the greenhouse for large, high-altitude greenhouses. In a greenhouse with a high eave height, there is more space for the heated air to rise from the bottom via buoyancy in summer; this results in a vertical temperature deviation. In particular, the temperature at the height of the crop zone could be lowered. It is necessary to quantitatively analyze the vertical temperature distribution inside the greenhouse due to the buoyancy effect and to analyze the reduction in temperature in the crop zone in summers, in the high-elevation greenhouse.

Therefore, in this study, the ventilation efficiency and temperature distribution in a CR-Venlo greenhouse during summer were evaluated according to the eave height. A computational fluid dynamics (CFD) program (FLUENT19.0, ANSYS, New York, NY, USA) was used to analyze various environmental conditions, such as the external wind speed. The internal air flow and ventilation efficiency of the CR-Venlo greenhouse were evaluated according to the external wind speed and eave height of the CR-Venlo greenhouse. This was followed by the evaluation of the ventilation effectiveness of a greenhouse with a high lateral elevation. The CR-Venlo greenhouse has a roof vent with both windward and leeward side openings; therefore, air flowing through the windward-side opening easily flows out through the opposite leeward-side opening. Therefore, two efficiencies were evaluated; one for air inflow through the roof vent and the other for air incoming into the greenhouse. Furthermore, the average temperature of the entire greenhouse and at the height of the crop zone was evaluated at varying external wind speeds and heights of the greenhouse. Finally, improved models with higher ventilation efficiencies than those in the CR-Venlo greenhouse are suggested based on ventilation efficiencies under the same environmental conditions for the CR-Venlo and C-Venlo greenhouses.

2. Materials and Methods

Figure 1 displays the research flow chart for this study. A CFD simulation model was designed to evaluate the ventilation efficiency of a CR-Venlo greenhouse. The standardized design of the CR-Venlo greenhouse was disseminated only recently; therefore, there are no

actual constructions. Lee et al. [14] evaluated the ventilation rate of the high-eave height 1-2W type 3-span Korean greenhouse in summer [14]. The CFD model information, such as crop module, turbulence model, and external area information, from this report was used in this study because both studies focus on the ventilation rate in greenhouses with high eave height in summer. However, previous study focused on the 1-2W and 3-span greenhouse, which is the most commonly used model in South Korea. Therefore, it was necessary to verify whether the information from the CFD simulation model [14] could be applied to other types of greenhouses; field experiments and verification of the simulation model were performed. The CFD model of the CR-Venlo greenhouse was designed, and the ventilation efficiency according to the eave height of the greenhouse was analyzed. First, the amount of air inflow and outflow through the roof vent were calculated according to the external wind speed and the eave height of the greenhouse were calculated. Next, the thermal environment of the CR-Venlo greenhouse was evaluated by calculating the average temperature of the entire greenhouse and the height of the crop zone. To address the limitations of the ventilation structure that uses only the roof vent of the CR-Venlo greenhouse, the possibility of improving ventilation efficiency by modulating the opening and closing of the roof vent and auxiliary facilities was evaluated.

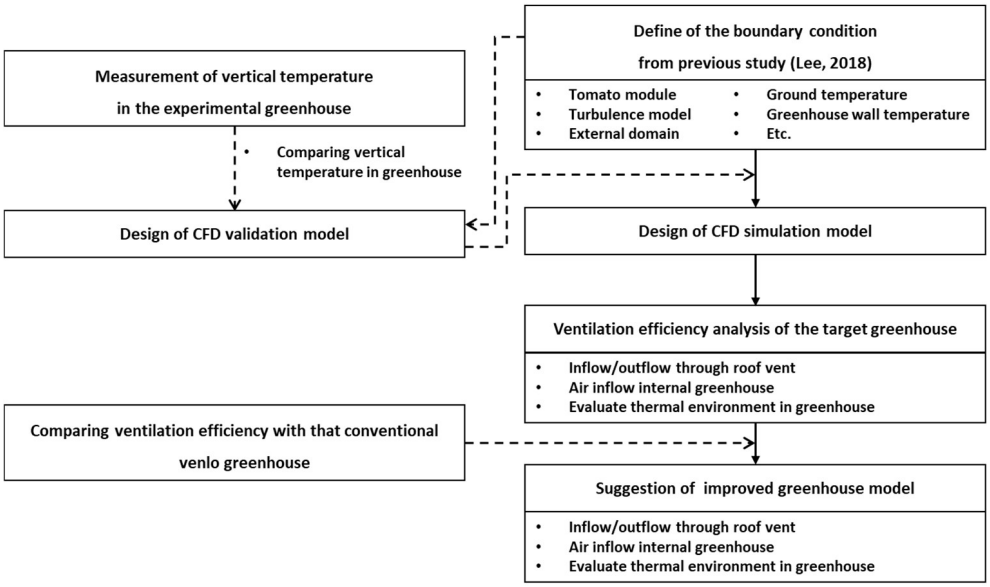

Figure 1. Flow chart of the experimental procedure.

2.1. Target Greenhouse

The CR-Venlo greenhouse, the target facility of this study, is an even-span greenhouse with a high eave height. It is like a C-Venlo greenhouse, but it has a large roof area with continuous roof windows (Figure 2). In this greenhouse, both the windward and leeward windows are open. It allows a lot of air to flow in and out through a large-area roof window and has excellent heat buffering capacity because of its large volume and ventilation rate due to a large-area roof window. Therefore, this type of greenhouse is beneficial in the cultivation of paprika and tomatoes in all seasons. A standard design of a CR-Venlo greenhouse has been developed; however, it has not yet been distributed to actual farms because of the lack of quantitative-analysis data on its ventilation efficiency. The CR-Venlo greenhouse in this study was designed based on the specifications presented in 19-Yeondong-3 (MAFRA, 2019) of the internal type of standard design drawing. The greenhouse length is 40.0 m; it is a 15-span greenhouse with a width of 8.0 m. The eave height is 7.0 m, and the ridge height is 1.1 m higher than the eave height. The covering of the greenhouse is 15.0 mm polyolefin film. The ceiling, side, front, and back of the greenhouse are all covered with film, and the floor is concrete. The roof vent of the CR-Venlo greenhouse is 1.0 m in width and 36.0 m in length. It has a large area of 39.4%

compared to approximately 14.7% of the total ceiling area of a C-Venlo greenhouse of the same volume. Ventilation is conducted by opening all roof windows by up to 45 degrees; a separate ventilation system was not considered, including side windows. In addition, a separate cooling system was not considered because the system was expected to have excellent thermal buffering capacity due to the high structural feature of the side elevation.

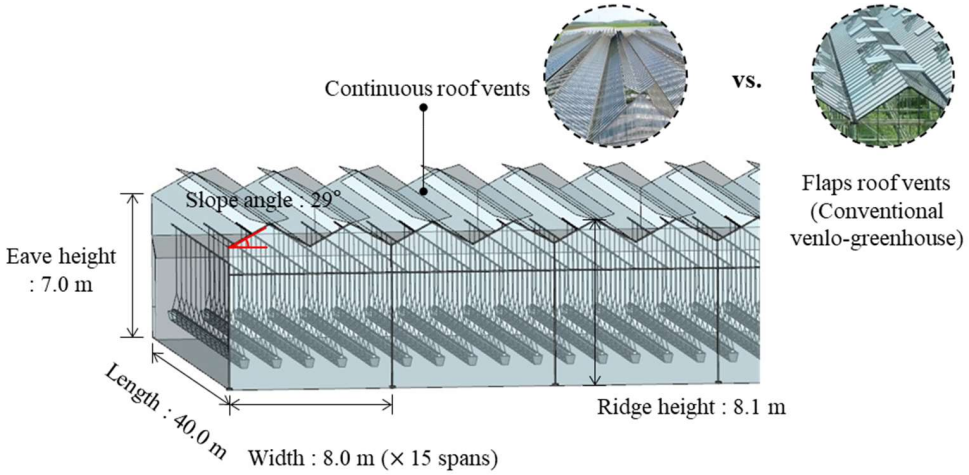

Figure 2. Schematic of a Korean Venlo-type greenhouse with continuous roof vents (MAFRA, 2019).

Tomatoes (*Solanum lycopersicum*), typically grown in domestic horticultural facilities, were chosen for cultivation in the target greenhouse. Tomato is conducive to continuous cropping through a hydroponics that reduces labor [19]. Five beds per span were arranged at 1.6 m intervals with two rows per bed (Figure 3). The beds were placed at 0.7 m from the ground; the width and height of the bed were 0.3 m and 0.15 m, respectively. A seedling cube with a width of 0.3 m and a height of 0.15 m was placed on the bed. The shape of the tomato crop was established as a cuboid with a width of 0.5 m and a height of 2.0 m.

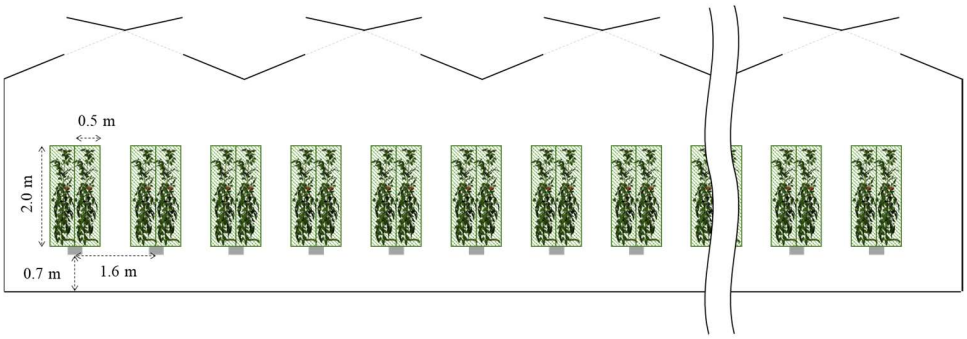

Figure 3. Schematic diagram of tomato arrangement in CFD simulation model.

2.2. Computational Fluid Dynamics (CFD)

Computational Fluid Dynamics (CFD) is a numerical analysis tool that can analyze fluid flow, heat transfer, and chemical action through computer simulation for a system containing a fluid. CFD uses the Navier-stokes equation, a nonlinear differential equation, as the governing equation. It is a tool for simulating numerical analysis using the finite difference method. It is actively used in various fields, including machinery, aviation, chemical engineering, manufacturing, civil engineering and construction, and environmental studies. It is applied in the agricultural field to evaluated livestock facilities and greenhouse environment [20–24].

In this study, a three-dimensional grid was designed using a commercial program for CFD (ver. 18.2, ANSYSInc, Canonsburg, PA, USA) to analyze the ventilation efficiency of the CR-Venlo greenhouse. The calculation was performed by setting boundary conditions

for the target domain. Fluent is a program that numerically analyzes the flow of fluid in an analysis space designed as a two- or three-dimensional grid, based on the law of conservation of mass, energy, and momentum. The equations used in the calculation are as follows:

$$\frac{\partial \rho}{\partial t} + \nabla \cdot \left(\rho \vec{v}\right) = S_m \tag{1}$$

$$\frac{\partial}{\partial t}\left(\rho \vec{v}\right) + \nabla \cdot \left(\rho \vec{v} \vec{v}\right) = -\nabla \mathrm{P} + \nabla \vec{\tau} + \rho \vec{g} + \vec{F} \tag{2}$$

$$\frac{\partial}{\partial t}(\rho E) + \nabla \cdot \left(\vec{v}(\rho E + P)\right) = \nabla \left(k_{eff} \nabla T - \sum h \vec{J_i} + \left(\vec{\tau}_{eff} \vec{v}\right)\right) + S_h \tag{3}$$

where ρ is the density of the fluid (kg·m^{-3}), $\vec{v}$ is the flow velocity of the fluid (m·s^{-1}), P is the static pressure (Pa), $\vec{\tau}$ is the stress tensor (Pa), and $\vec{g}$ is the acceleration due to gravity. (m·s^{-2}), $\vec{F}$ is the external force (N·m^{-3}), S_m is the source term of the mass (kg·m^{-3}), k_{eff} is the effective conductivity (kg·m^{-2}·s^{-1}), T is the temperature (K), E is the specific enthalpy indicating the enthalpy per unit mass (J·kg^{-1}), t is the time (s), $\vec{J_i}$ is the diffusion flux of type **i** (kg·m^{-1}·s^{-1}), and S_h is the total enthalpy (kg·m^{-1}·s^{-3}).

2.3. Experimental Procedure

2.3.1. Field Experiment and Modelling for Validation of the CFD Simulation Model

A field experiment was conducted to verify the simulation model for a wide-span type greenhouse using roof vents similar to those in the structure of the CR-Venlo greenhouse (Figure 4). The target greenhouse is a 5-span wide type greenhouse located in Moga-myeon, Icheon-si, Gyeonggi-do (37°18′N, 127°48′E). The dimension of the 1-span of target greenhouse was a width of 9 m, a length of 30.0 m, an eave height of 3.5 m, and a ridge height of 5.5 m. The tomato (*Solanum lycopersicum*) was grown hydroponically inside the target greenhouse. The planting density was approximately 3 plants·m^{-2}, and the plants were cultivated in the one-stem attraction method. Tomatoes were approximately 60 days old during the experiment. The cultivation environment was controlled by ventilation using roof vents based on the values obtained using the central temperature sensor. The temperature was maintained at 24–26 °C, which is the optimal growing temperature for tomatoes. The field experiment was conducted on 8 July 2020, and the vertical temperature distribution was measured for six points (0.8–4.8 m) at 0.8 m height intervals regarding the central location of the greenhouse. The internal air temperature was measured at 1 s intervals using a Type-T thermocouple; the measured data was processed to obtain a 10 s average value.

The CFD model for validation was designed for the greenhouse on which the field experiments were performed. The model information, including the turbulence model and grid size, was like that of the CFD model of the CR-Venlo greenhouse. External weather data, such as wind direction, wind speed, and air temperature, were obtained from the Ochang Meteorological Observatory, the closest meteorological station. The external weather data of the period in which the vertical wind (±15°) blows against the sidewall of the greenhouse, and the average values of the wind speed and air temperature were used. Tomatoes in the mature stage exchange sensible and latent heat and act as resistance to airflow. Therefore, the CFD model was designed based on the values of a previous study for a mature tomato plant [25] (Table 1).

Figure 4. Experimental greenhouse located in Moga-myeon, Icheon-si, Gyeonggi-do Province (37°18′N, 127°48′E) and field experiment (**a**) External view of the experimental greenhouse, (**b**) Sensor installation for measuring vertical air temperature, (**c**) Internal view of the experimental greenhouse and (**d**) Sensor installation to avoid direct radiation.

Table 1. Values of the boundary condition of the CFD simulation model for validation.

Boundary Condition		Input Values	Reference
Outside air temperature (°C)		27.4	Field experiment and Ochang weather station (Average value during field experiment period)
Wind speed ($m \cdot s^{-1}$)		1.40	
Wind direction (°)		90	
Greenhouse wall	Temperature (°C)	27.4	
	Thickness (m)	0.0001	
Tomato	Latent energy sources ($W \cdot m^{-3}$)	−30.0	Lee [25]
	Viscous resistance (m^{-2})	2.53	
	Inertial resistance (m^{-1})	1.92	
Turbulence model		Realizable k-ε	

2.3.2. Design of External Domain and Wind Environment of the CFD Simulation Model

The external wind environment is an important factor in calculating the natural ventilation rate. The wind speed and the turbulence distribution by height vary depending on the stability of the atmosphere. Therefore, to apply these conditions to the CFD model,

the average profiles of wind-speed, turbulence-energy, and turbulence-dissipation-rate were calculated through the conditional equations reported earlier; a user-defined function was created as a code and was reflected in the model [26,27]. The flow velocity profile and turbulence profile applied to CFD in the external wind environment are as follows:

$$u(z) = \frac{u^*_{ABL}}{k} \ln\left(\frac{z + z_0}{z_0}\right), \quad (4)$$

$$\varepsilon(z) = \frac{{u^*_{ABL}}^3}{k(z + z_0)}, \quad (5)$$

$$\omega(z) = \frac{\varepsilon}{C_\mu k}, \quad (6)$$

where u is the wind speed at height z ($m \cdot s^{-1}$), u^*_{ABL} is the friction velocity ($m \cdot s^{-1}$), k is the Kármán constant (dimensionless), z_0 is the roughness length (m), ε is the turbulent energy dissipation ($m^2 \cdot s^{-3}$), ω is the specific dissipation rate (s^{-1}), and C_μ is the empirical constant (dimensionless).

Until recently, there was no detailed standard for designing the external domain of a 3D computational fluid dynamics model; approximate values had been suggested through empirical or experimental verification [28–30]. Kim et al. [31] proposed the minimum length of the outer region where the atmospheric boundary layer reaches the center based on the height of the target building, to prevent the internal boundary layer from continuously growing [31]. The size of the entire computational domain can be determined by the height of the study object. If there is an object larger than the study object, it should also be considered. The vortex formed at the highest point dissipates at the farthest point within the analysis domain.

Therefore, in this study, the external area for natural ventilation was designed based on the results of previous research [31]; the length of the upstream section on the windward side was set at 3H. The side and upper surfaces of the analysis area were designed to be 5H each in a range where the vortex formed from the greenhouse does not affect them. The length of the downstream section was designed to be 15H considering the convergence and economic feasibility. The size of mesh inside the greenhouse was 0.3 to 0.5 m, and the total number of meshes was approximately 8.1 million (Figure 5).

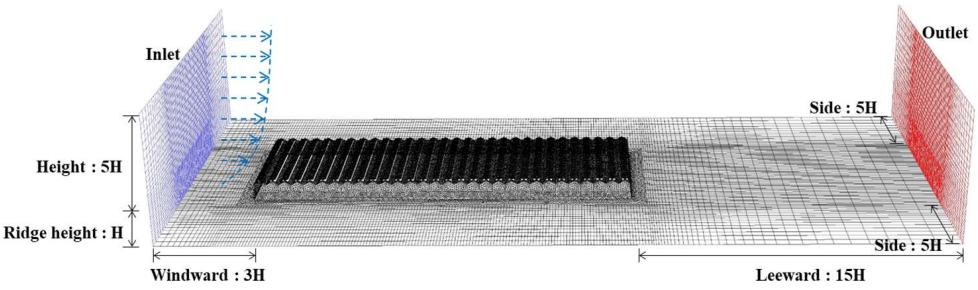

Figure 5. Design of the CFD simulation model domain.

2.3.3. Boundary Conditions of the CFD Simulation Model

The 3D simulation model of the CR-Venlo greenhouse was designed referring to the 19-Yeondong-3 model of the standard design [1] and was designed for five eave heights to analyze the ventilation efficiency at different eave heights of the greenhouse. The simulation target period was established for the hot summer season, the temperature of the outside air was set to 35 °C, which corresponds to 1% of the TAC (Technical Advisory Committee) temperature of the summer weather data (1990–2020) for the last 30 years in Daegu. The turbulence model, the size of grid, and boundary conditions such as internal ground temperature, sensible heat, and latent heat of tomato were designed referring to the modeling conditions of a previous study [25] (Table 2).

Table 2. Boundary condition values of the CFD simulation model for case study.

Boundary Condition		Input Values	Reference
Outside air temperature (°C)		35.0	Weather station data (1990-2020) and
Greenhouse wall	Temperature (°C)	35.0	
	Thickness (m)	0.0001	MAFRA (2019)
Ground temperature inside the greenhouse (°C)		45.0	Lee [25]
Ground temperature outside the greenhouse (°C)		44.16	
Tomato	Latent energy sources ($W \cdot m^{-3}$)	−30.0	
	Viscous resistance (m^{-2})	2.53	
	Inertial resistance (m^{-1})	1.92	
Turbulence model		Realizable k-ε	

2.3.4. Analytical Conditions for Evaluation of Ventilation Efficiency

When the external wind speed is over 2.0 $m \cdot s^{-1}$, wind-driven ventilation is dominant; when the external wind speed is less than 0.5 $m \cdot s^{-1}$, gravity with buoyancy driven ventilation is dominant [4,32]. Depending on the wind speed, there are variations in the main factors that affect the ventilation efficiency of natural ventilation. The wind speed at which wind-driven ventilation and buoyancy-driven ventilation are predominant differ with the number and size of the peristaltic ventilation of the greenhouse. Therefore, in this study, the external wind speed conditions at the height of the greenhouse eave were established at 0.5, 1.5, and 3.0 $m \cdot s^{-1}$ to include both conditions where buoyancy-driven ventilation and wind-driven ventilation are dominant for the CR-Venlo greenhouse. Wind direction conditions were subjected to a 90° wind perpendicular to the length of the greenhouse. To analyze the changes in the ventilation rate with the height of the CR-Venlo greenhouse, 15 case simulation models were analyzed for different measured heights of the greenhouse (5, 6, 7, 8, and 9 m) (Table 3).

Table 3. Analysis cases for the evaluation of ventilation efficiency using the CFD simulation model.

Analysis Cases	Conditions
Wind direction (°)	90
Wind speed ($m \cdot s^{-1}$)	0.5, 1.5, 3.0 (at the roof height of the greenhouse model)
Rigid height of the greenhouse	5, 6, 7, 8, 9
Total	15 cases

The CR-Venlo greenhouse is expected to have high ventilation because of the large area of the roof vent window. However, the inflow air immediately flows out because the windward and leeward roof windows facing each other are open. Therefore, in wind-driven ventilation conditions in which air inflow and outflow through the roof window are actively performed, ventilation efficiency could be reduced. To overcome the limitations of the ventilation structure, an improvement is proposed by analyzing the opening and closing of each roof window in the CR-Venlo greenhouse and the natural ventilation efficiency, based on the installation of auxiliary facilities under wind-driven ventilation conditions (3 $m \cdot s^{-1}$) (Figure 6 and Table 4). To strengthen the main airflow according to the location of each span, Case 1–3 models were proposed in which the roof windows in the windward and leeward direction were all opened according to the location of the 15 span greenhouses. In addition, the airflow toward the bottom of the greenhouse was strengthened by installing a virtual windbreak at the mid-point of the roof window or by increasing the roof opening angle.

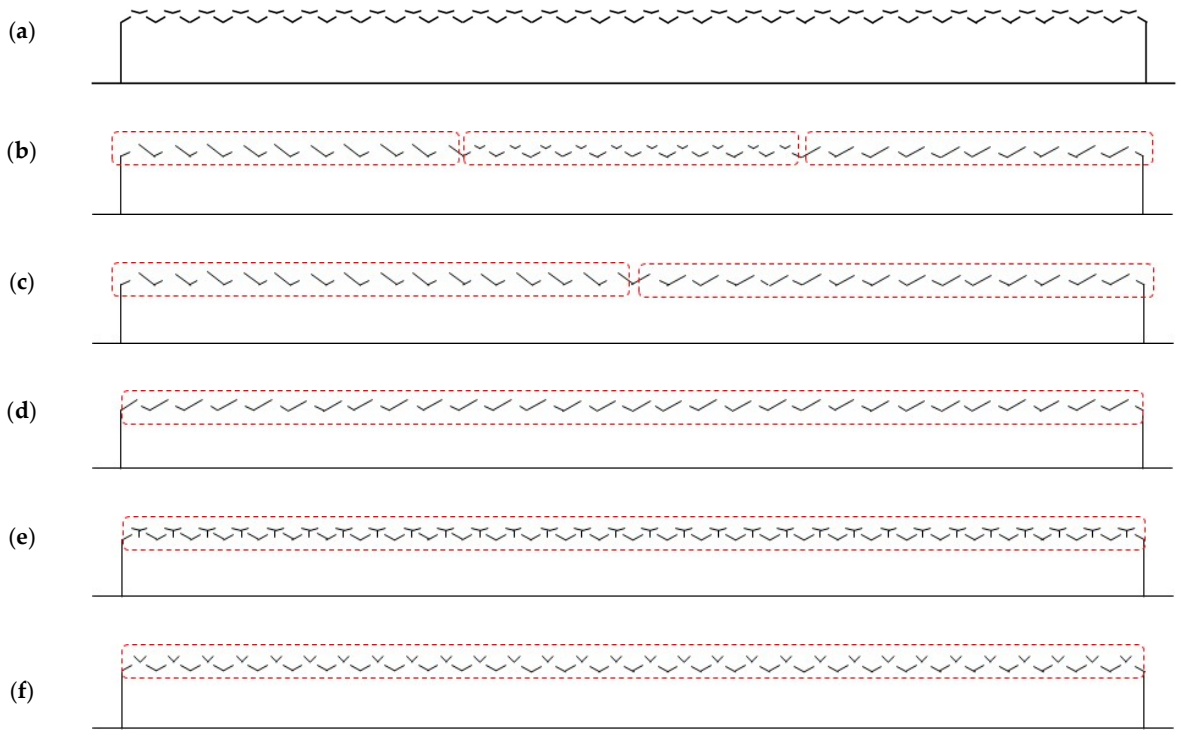

Figure 6. Schematic depicting the improved model ventilation structure of the CR-venlo greenhouse with continuous roof vents: (**a**) Case 0: CR-venlo greenhouse, (**b**) Case 1: Opening of windward roof vents at 1–5 span and leeward roof vents at 11–15 span, (**c**) Case 2: Opening of windward roof vents at 1–7.5 span and leeward roof vents at 7.5–15 span, (**d**) Case 4: Opening of all windward roof vents, (**e**) Case 4: Windbreak installation in the center of all roof vents, (**f**) Case 5: Increasing the opening angle of roof vents.

Table 4. Specifications of the modified CFD simulation model to improve ventilation rate.

Model	Installation of Wind Break in the Roof	Opening Condition of Roof Vents	Opening Angle of Roof Vents (°)
Case 0	X	All spans: Open on both windward and leeward sides	45
Case 1	X	1–5 spans: Open on the windward side 6–10 spans: Open on both windward and leeward sides 11–15 spans: Open on leeward side	45
Case 2	X	1–7.5 spans: Open on windward side 7.5–15 spans: Open on leeward side	45
Case 3	X	All spans: Open on leeward side	45
Case 4	O	All spans: Open on both windward and leeward sides	45
Case 5	X	All spans: Open on both windward and leeward sides	75

2.3.5. Evaluation of Ventilation Efficiency and Thermal Environment

A large amount of fresh outside air should flow into the greenhouse, and the heated air inside the greenhouse should be smoothly discharged to the outside. The CR-Venlo greenhouse does not have a side window and can only be ventilated through the roof window; the inlet and outlet have the same structure. In addition, the distance between the roof windows is considerably short, and all the facing roof windows are open. The air introduced through the roof window can immediately flow out through the facing roof

window. Therefore, it is necessary to evaluate whether fresh air is introduced into the greenhouse through the roof window and whether it replaces the air inside the greenhouse.

In this study, the ventilation efficiency through the roof window of the CR-venlo greenhouse was evaluated by calculating the air inflow and outflow through the roof vent of each span (Figure 7a). Based on the roof window surface of the greenhouse, the inside direction was designated as '+' and the outside direction as '−'. Air inflow through the greenhouse roof window (Air_{inflow}) was calculated as the mass flow rate in the positive direction ((①+②)/2) and air outflow through the greenhouse roof window ($Air_{outflow}$) was calculated as the mass flow rate in the negative direction ((③+④)/2). The air introduced through the roof window that flows into the interior space of the greenhouse was assessed by defining a virtual reference plane parallel to the floor of the greenhouse in the area near the roof of the greenhouse and by calculating the mass flow rate (⑤) of the air that flows into the interior of the greenhouse (Figure 7b). Figure 8 indicates the position of each span where the ventilation efficiency was calculated.

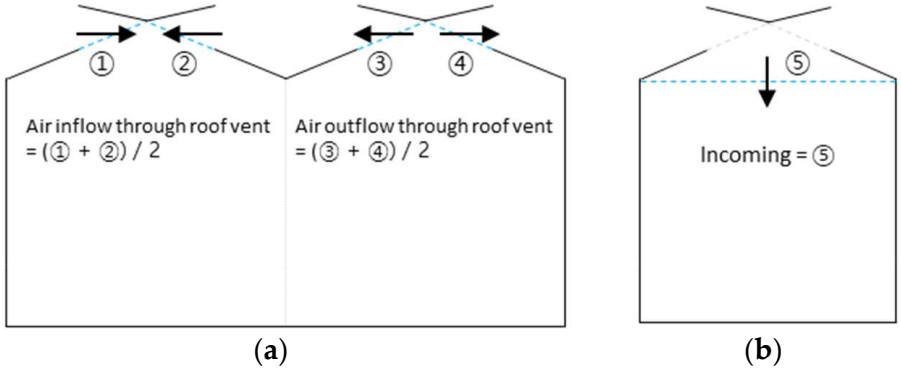

Figure 7. Schematic diagram of the evaluation of air inflow/outflow through the roof vent and the incoming air inflow. (**a**) Evaluation of air inflow/outflow through the roof vent, (**b**) Evaluation of incoming air inflow.

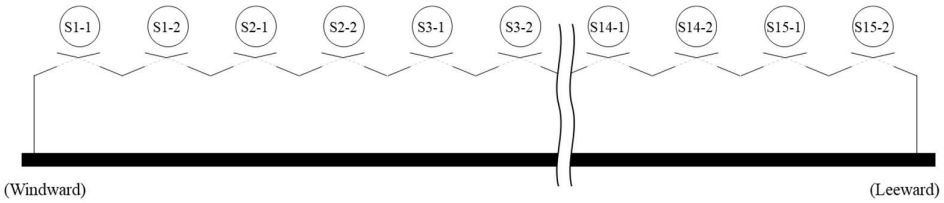

Figure 8. Region definitions for Korean Venlo-type greenhouses with continuous roof vents used to evaluate ventilation efficiency.

The design of the CR-Venlo greenhouse is expected to decrease the temperature of the lower part of the greenhouse by allowing hot air to rise to the upper part of the greenhouse during summer due to the high elevation of the structure. Therefore, the reduction in air temperature at different heights of the greenhouse was analyzed. The average air temperature at different heights of the greenhouse, was also calculated, and the average air temperature at the height of the tomato crop zone (0.7–2.7 m), which directly affects the growth of the crops.

3. Results

3.1. Validation of the CFD Simulation Model

To verify the CFD simulation model, the changes in the vertical temperature inside the greenhouse with changes in the external weather conditions were measured for a wide-span greenhouse (Figure 9). In the case of the field experiment, the wind direction, wind speed, and the external temperature continuously changed. The CFD model in this

study analyzed the ventilation rate of the greenhouse for each wind direction and wind speed condition; therefore, the analysis was performed assuming a steady-state. The data measured at constant wind direction and blowing time among the experimental field data were used for validation. The wind direction (246° ± 15°) that is perpendicular to the sidewall of the greenhouse, which can effectively influence the change in temperature inside the greenhouse due to the inflow of external air, the blows, and the data for the time (PM 12:20) of high external air was used. The external wind speed was 1.4 $m \cdot s^{-1}$.

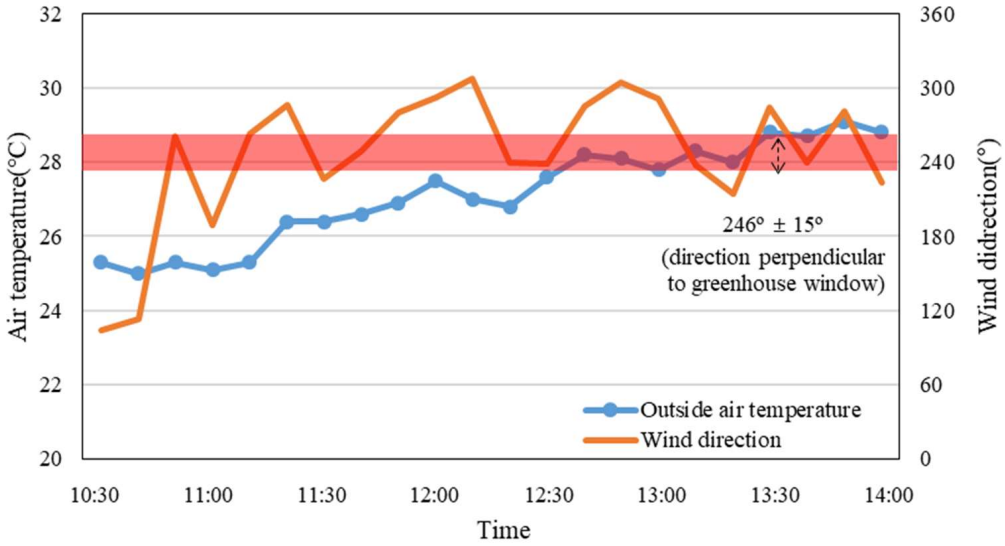

Figure 9. The outside air temperature and wind direction in the experimental greenhouse located in Moga-myeon, Icheon-si, Gyeonggi-do Province (37°18′N, 127°48′E) during the experimental period (July 2020).

The data measured through the field experiment change in real time despite using 10 s average data measured for 1 min for a relatively constant time under a specific wind direction and speed; therefore, the changes in the internal vertical temperature profile with the measurement time were evaluated (Figure 10). The temperature profile exhibited a tendency to change the temperature at the top height. It was influenced by wind conditions changing in real-time. According to the wind conditions, the influence of outside air entering the greenhouse through the roof window was variable. In the CFD verification model, the simulation was performed assuming a steady state; therefore, the location where the outside air is introduced through the roof vent and the location where the air inside the greenhouse flows out are divided according to the span location of the greenhouse. A constant vertical temperature profile was calculated according to the span position of the greenhouse. In the central position of the greenhouse, which is the verification position, the internal temperature exhibited a tendency to increase as the height of the greenhouse increased.

In field experiments and simulation results for comparative verification, because field experiments were conducted at the central location of the greenhouse, the simulation calculation results of the same location were used. The CFD verification model was validated; therefore, it exhibited a similar trend to the field test result and the shape of the vertical temperature profile at the central location of the greenhouse (RMSE: 0.3 ~ 1.1 °C; R^2: 0.88~0.99); it predicted the vertical temperature inside the greenhouse by roof-window ventilation.

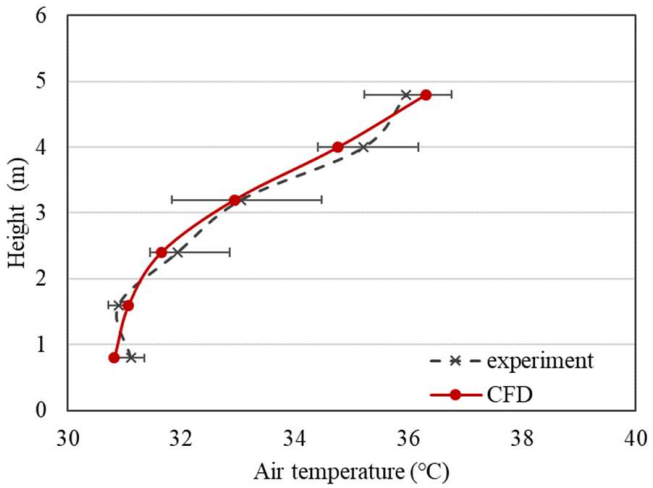

Figure 10. Validation of the CFD simulation model for the vertical temperature in the greenhouse. (The error bar of the field experiment in the unsteady state means the range of the maximum and minimum values).

3.2. Evaluation of Air Inflow and Outflow Rate through Roof Vent According to Wind Speed

3.2.1. Analysis of Airflow Pattern According to Wind Speed

A single or multi-span greenhouse where the number of spans is not large is greatly affected by wind ventilation when the external wind speed is 2.0 m·s^{-1} or higher, whereas large-scale greenhouses with many spans are relatively less affected by wind ventilation [8]. The target is a large greenhouse with a high side elevation and 15 spans; therefore, the conditions that predominantly affect ventilation according to the wind speed would be different. In case of simulation calculations for a low wind speed (0.5 m·s^{-1}), the flow inside the greenhouse is formed according to the external air inflow and an upward airflow from the floor is formed due to buoyancy. (Figure 11). Therefore, gravity with buoyancy driven ventilation is dominant. With simulation results for high wind speed (1.5 and 3.0 m·s^{-1}) there is no upward airflow due to buoyancy on the windward side. The flow of air introduced from the roof window reached the bottom of the crop and greenhouse, and the internal airflow was majorly formed.

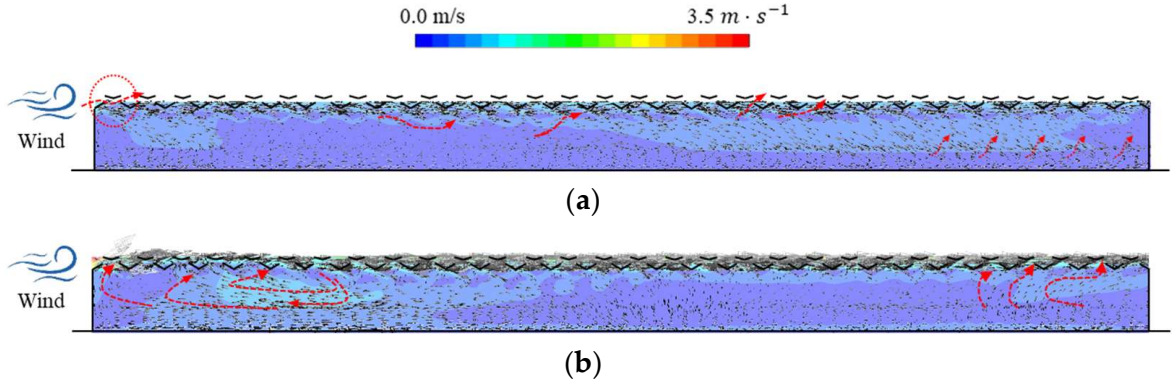

Figure 11. CFD computed airflow distribution at the center of the cross section of the greenhouse according to the external wind speed (the external wind direction was fixed perpendicular to the side window). (**a**) Airflow distribution in the eave height 7m and external wind speed 0.5 m · s^{-1} (Center cross section of the greenhouse). (**b**) Airflow distribution in the eave height 7 m and external wind speed 3.0 m · s^{-1} (Center cross section of the greenhouse).

Here, wind ventilation dominates, and below 0.5 m·s^{-1}, gravity with buoyancy driven ventilation dominates; as the number of spans increases, the effect of gravity with buoyancy driven ventilation increases. In the greenhouse case of the inside on the downwind side, the

influence of the air flowing in from the outside was relatively reduced; therefore, an updraft was formed because of buoyancy. The ventilation efficiency of the Korean-style interlocking greenhouse was evaluated according to the wind-environment conditions because the main mechanisms affecting greenhouse ventilation varied with the wind speed conditions.

3.2.2. Estimation of Inflow/Outflow Rate at Roof Vent

The inflow/outflow rate through the roof vents of the CR-Venlo greenhouse according to the external wind speed was quantified (Figure 12). The calculation of the airflow rate passing through the roof vents of the CR-Venlo greenhouse under low wind speed (0.5 $m \cdot s^{-1}$) conditions for each span revealed that the highest air inflow ($\mathbf{Air_{inflow}}$) was in the first span on the windward side with 14.99 $kg \cdot s^{-1}$, and the air inflow gradually decreased toward the leeward side. The air outflow ($\mathbf{Air_{outflow}}$) through the greenhouse roof vent in each span was greater on the windward side and decreased toward the leeward side. Under low (0.5 $m \cdot s^{-1}$) and high wind speed (3.0 $m \cdot s^{-1}$) conditions, the coefficient of variation (CV) for the air outflow through the greenhouse roof vents was 28.4% and 32.5%, respectively. Therefore, under low wind-speed conditions, the overall air outflow is uniform for all spans, and indirectly indicates that the airflow inside the greenhouse is predominantly influenced by gravity with buoyancy driven ventilation.

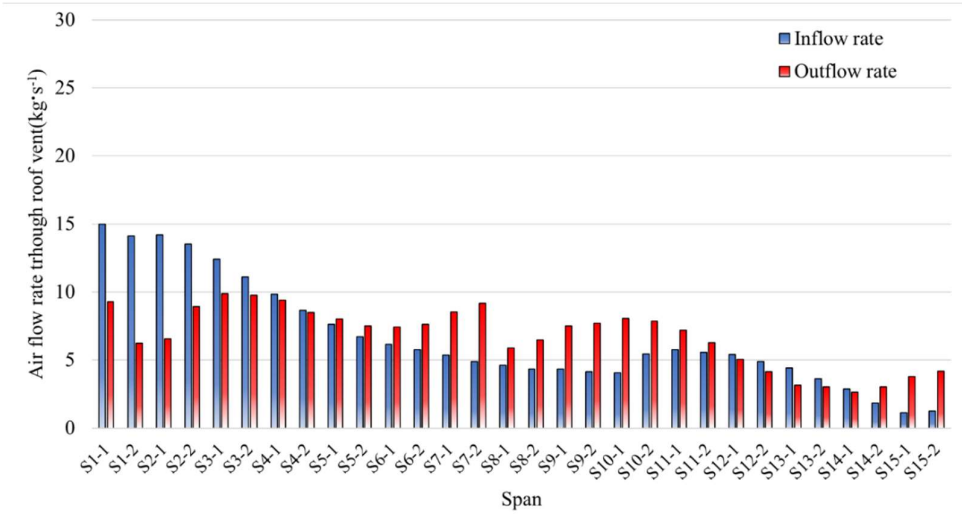

(**a**)

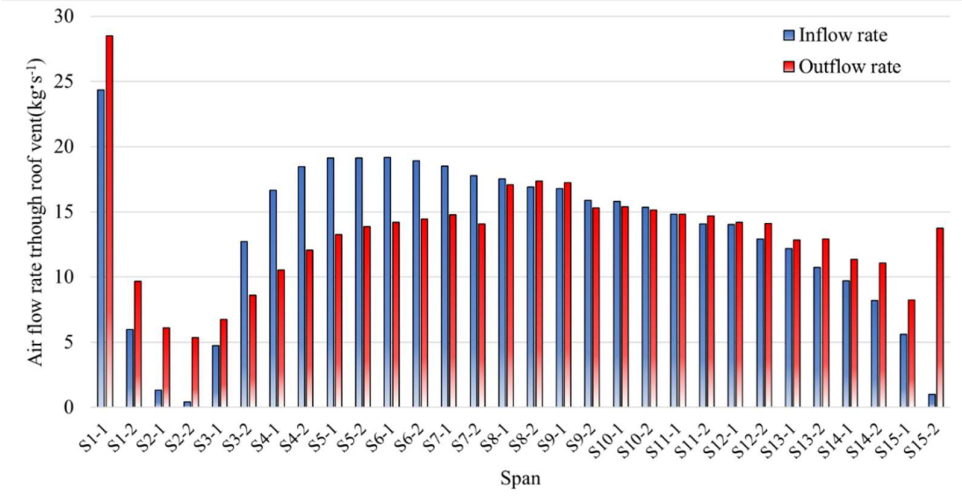

(**b**)

Figure 12. Air inflow and outflow through roof vent with 7 m eave height according to wind speed. (**a**) External wind speed 0.5 $m \cdot s^{-1}$, (**b**) External wind speed 3.0 $m \cdot s^{-1}$.

The calculation of the flow rate for air passing through the greenhouse roof vents at high wind speed for each span revealed that the first span on the windward side had the highest air inflow ($\mathbf{Air_{inflow}}$) with 24.35 kg·s^{-1}, and the air outflow ($\mathbf{Air_{outflow}}$) was also high with 28.53 kg·s^{-1}. Except for the first span, little air flowed through the roof vents in spans on the windward side, and after the span in the center of the greenhouse, air inflow rate through the roof vents increased to approximately 80% of that of the first span. This was because most of the air flowed in through the first span on the windward side, and the airflow separation was largely generated by the greenhouse structure at first span. The inflow through the roof vents gradually decreased toward the spans on the leeward side, and the air outflow rate was greater than that of the inflow. In particular, the volume of outflow from the last span on the leeward side was four times that of the inflow, indicating that the outflow of internal air was dominant at the leeward side.

3.2.3. Estimation of Incoming Flow Rate

The volume of inflow and outflow through the roof vent indicates the ventilation efficiency of the CR-Venlo greenhouse roof vent; however, it does not guarantee to increase the ventilation rate at the height of the crop zone in the CR-Venlo greenhouse. Because all facing roof vents on the same span are open and the distance between roof vents is considerably short; most air escapes through the roof vent on the opposite side in the case of ventilation under high external wind speed (Figure 13). Therefore, quantitative evaluation of air inflow through the roof vent is necessary to determine if air actually flows into the greenhouse. To quantitatively compare this, a CFD model for the general Venlo greenhouse, which has the same shape as the CR-Venlo greenhouse but with a different roof vent, was created. Ventilation efficiency was compared, and the volume replacement rate per minute was calculated (Table 5). The volume replacement rate per minute in the CR-Venlo greenhouse under low wind-speed conditions (0.5 m·s^{-1}) was 0.17 AER min^{-1}, which was higher than that in the European-style Venlo greenhouse (0.10 AER min^{-1}). The volume replacement rate per minute of the CR-Venlo greenhouse under high wind-speed conditions (3.0 m·s^{-1}) was 0.28 AER min^{-1}, which was lower than that in the European-style Venlo greenhouse (0.49 AER min^{-1}). The CR-Venlo greenhouse has a structure similar to that of the European-style Venlo greenhouse, but the CR-Venlo greenhouse has a relatively large area of roof window. It means that the large roof window area of the CR-Venlo greenhouse helps gravity with buoyancy driven ventilation very efficiently under low wind speed conditions. In high wind speed conditions, where the influence of wind-driven is ventilation high, ventilation through the wide roof window area was not effective. This result contradicts the results obtained when much of the external air flows through the roof window of the CR-Venlo greenhouse, indicating that the influx of external air through the roof window was ineffective.

The ventilation efficiency was evaluated considering the characteristics of a CR-Venlo greenhouse vent; the total inflow of external air through the roof vent and actual air inflow ($Air_{incoming}$) into the greenhouse was assessed.

Table 5. CFD computed ventilation rates based on the MFR method of the CR-Venlo greenhouse and C-Venlo greenhouse.

External Wind Speed (m·s^{-1})	Air Exchange Rate Per Minute (AER min^{-1})	
	Venlo-Type Greenhouse with Continuous Roof Vent Open	Conventional Venlo-Type Greenhouse
0.5	0.17	0.10
3.0	0.28	0.49

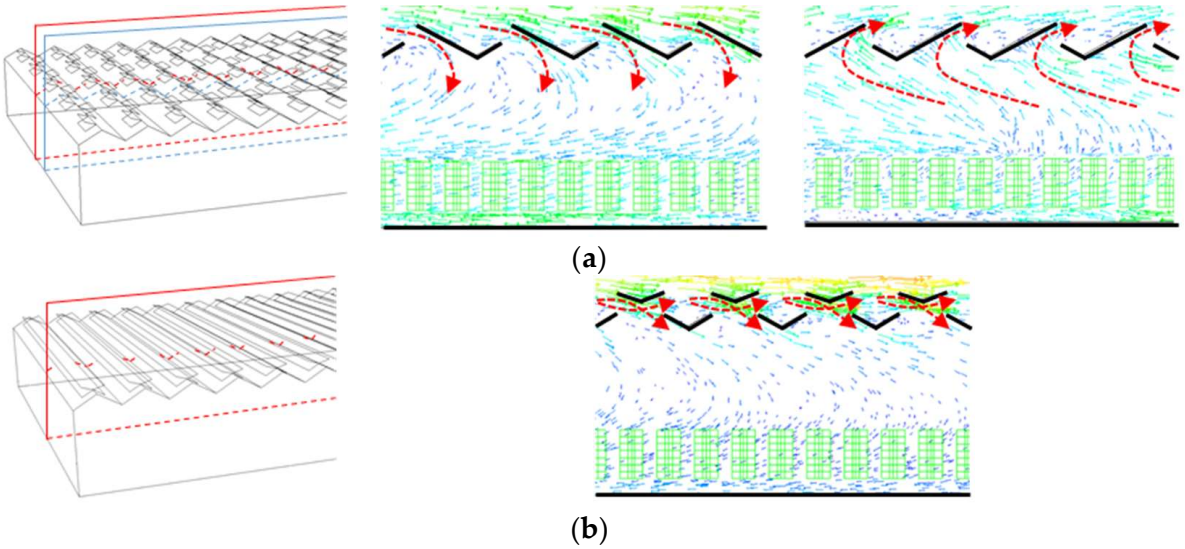

Figure 13. Airflow in middle span of the greenhouse with a ridge height of 7 m under the external wind speed of 3 m·s^{-1}. (**a**) Airflow pattern of Dutch Venlo-type greenhouse through the roof vents, (**b**) Air flow pattern of Korean Venlo-type greenhouse through the roof vents.

The top graph in Figure 14a depicts the air inflow (Air_{inflow}) through the roof vent at various heights of the greenhouse at an external wind speed of 0.5 m·s^{-1}, and the bottom graph indicates the air inflow ($Air_{incoming}$) through the roof window. On the top graph, the efficiency of inflow of external air in each span in the greenhouse can be evaluated, and on the bottom graph, the efficiency of the air flow out of the greenhouse can be evaluated. The mass inflow rate (Air_{inflow}) was higher in the span on the windward side, where the inflow of external air begins. It gradually decreased toward the spans on the leeward side. Air flowing into the greenhouse ($Air_{incoming}$) was higher in the span on the windward side and gradually decreased toward the spans on the leeward side. The air inflow in each span changed gradually and the airflow separation in the first span in the greenhouse was not severe. This could be attributed to the dominant gravity with buoyancy driven ventilation because the external wind speed was relatively low. The air flow into the greenhouse, compared to the mass inflow rate through the roof vent in the greenhouse, presented at 30.3–61.4% in most spans, except for the span on the windward side (81.0~100%).

Figure 14c depicts the air inflow (Air_{inflow}) through the roof vent at different heights of the greenhouse under an external wind speed of 3 m·s^{-1}, as well as the air flow into the greenhouse ($Air_{incoming}$). With the first and second spans on the windward side, which had high levels of mass inflow rate, most air did not flow into the greenhouse. The ratio of air that actually flowed into the greenhouse was less than 2%, with most air (98%) flowing out of the greenhouse. Furthermore, most of the spans, except for the first and second spans on the windward side and the last span on the leeward side, exhibited an air inflow efficiency of 12.55–34.41%. Therefore, although the mass replacement rate was high due to the opening of all facing roof vents, the actual air inflow efficiency was not.

When the height of the greenhouse increased, the ratio of air that flowed into the greenhouse improved by a maximum of 4.59% in the span at the center of the greenhouse. This indicates that airflow separation that occurs on the sidewall on the windward side was greater, and consequently, the air inflow efficiency in the span in the center of the greenhouse increased. However, in most greenhouse spans, the improvement of air inflow efficiency with the height of the greenhouse was minimal, ranging from 0.16 to 3.50%. Therefore, improvements are necessary to allow a lot of air to enter the greenhouse through the roof vent.

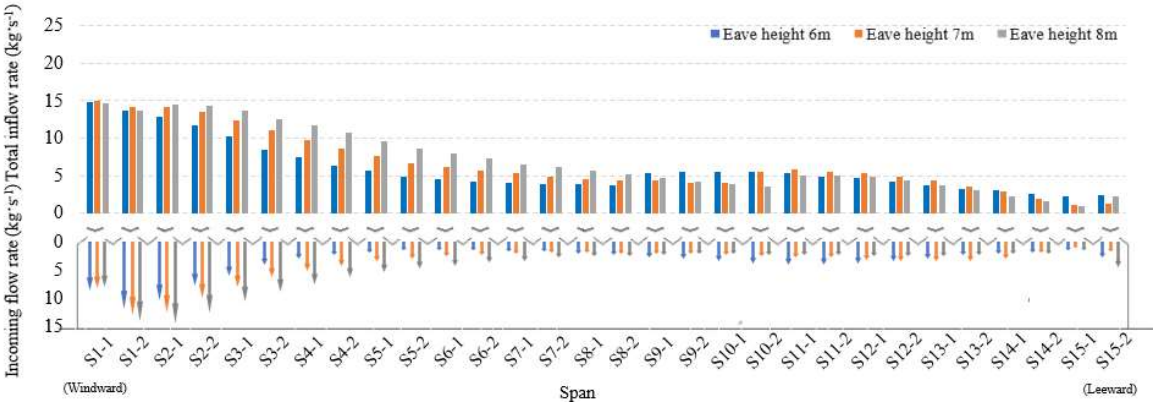

(**a**)

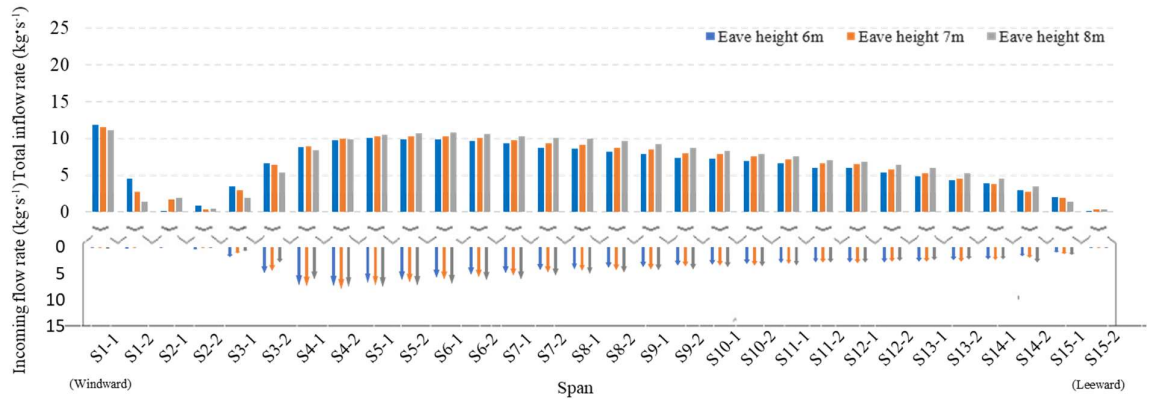

(**b**)

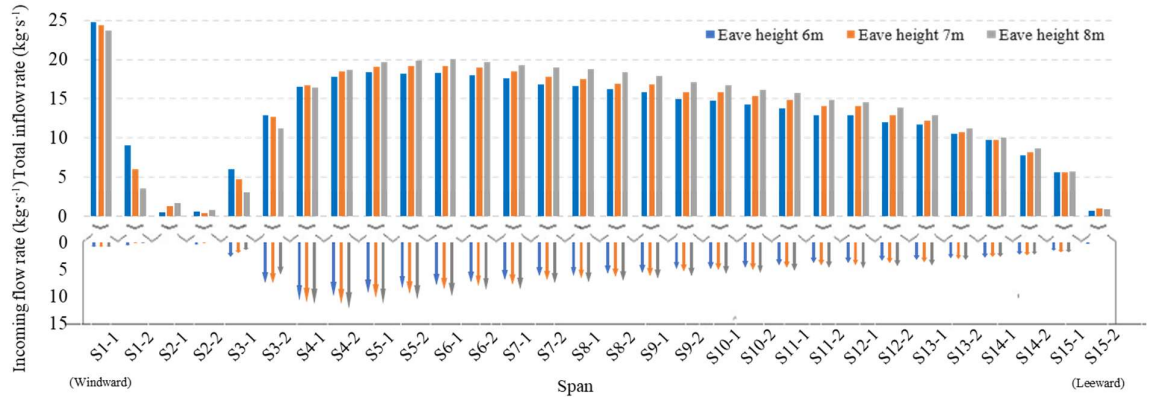

(**c**)

Figure 14. Total inflow rate and incoming flow rate according to the eave height and external wind speed. (**a**) External wind speed 0.5 m · s^{-1}, (**b**) External wind speed 1.5 m · s^{-1}, (**c**) External wind speed 3.0 m · s^{-1}.

3.3. Evaluation of the Thermal Environment of the Greenhouse According to the Height of the Eave

The thermal environment analysis of the CR-Venlo greenhouse revealed that, except for the first span, the temperature increased as the internal height of the greenhouse increased in the spans on the windward side (Figure 15). The amount of air entering the roof vent is small; however, the amount of internal air flowing out was dominant in these spans. For the central span, the temperature increased with increasing internal height of the greenhouse; however, the temperature decreased after a certain height. The inflow of air separated from the sidewall on the windward side through the roof vent after the central span possibly lowers the temperature at the top of the greenhouse. With the leeward side span, the higher

the location inside the greenhouse, the higher the temperature. The dominant amount of external air inflow in the central span of the greenhouse moving toward the spans on the leeward side and flowing out through the roof vents have caused this.

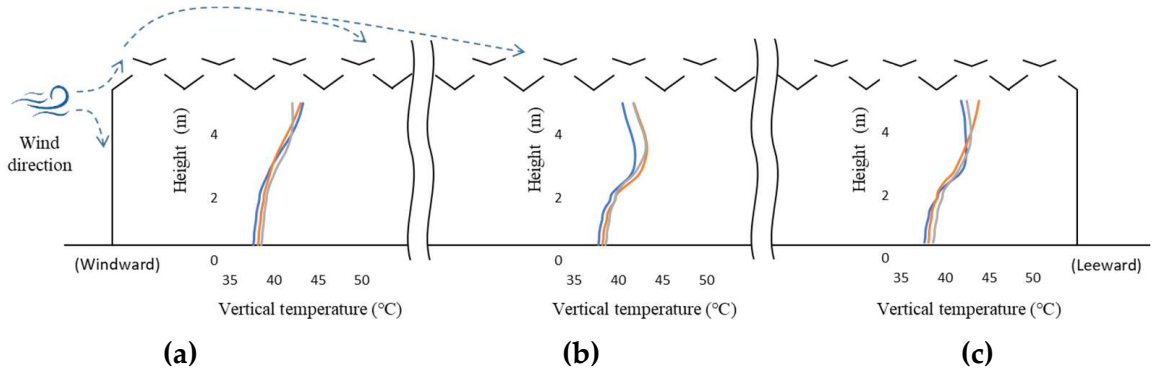

Figure 15. Vertical temperature profile of greenhouse according to the external wind speed (— 0.5 m·s^{-1} — 1.5 m·s^{-1} — 3.0 m·s^{-1}). (**a**) 1~5 span, (**b**) 6~10 span, (**c**) 11~15 span.

Analysis of average greenhouse temperature and crop zone temperature at different heights of the CR-Venlo greenhouse revealed that the higher the height of the greenhouse, the lower was the average greenhouse temperature and crop zone temperature, under all wind conditions (Figure 16). This could be attributed to the increased volume of the greenhouse, combined with the increase in the greenhouse height. This causes hot air to move to the upper part of the greenhouse, resulting in the rapid removal of heat. These results are in line with those in earlier reports [1]. However, when the external wind speed was 1.5 m·s^{-1}, the amount of temperature decrease with increasing greenhouse height was reduced. The temperature of the crop zone decreased by 0.6 °C when the greenhouse height was 6 m compared to that at 5 m; it decreased by 0.1 °C when the height was 9 m compared to that at 8 m. This may be due to the low efficiency of the flow of external air into the greenhouse because in the ventilation structure of the CR-Venlo greenhouse, all facing roof vents are open. When the height of the greenhouse increases, the heated air on the floor of the greenhouse should move up and escape to the outside through the roof vent; the efficiency of hot air removal is influenced by the low efficiency of ventilation through the roof vent. Consequently, the overall temperature of the internal greenhouse and the crop zone decreased slightly with increasing height of the CR-Venlo greenhouse.

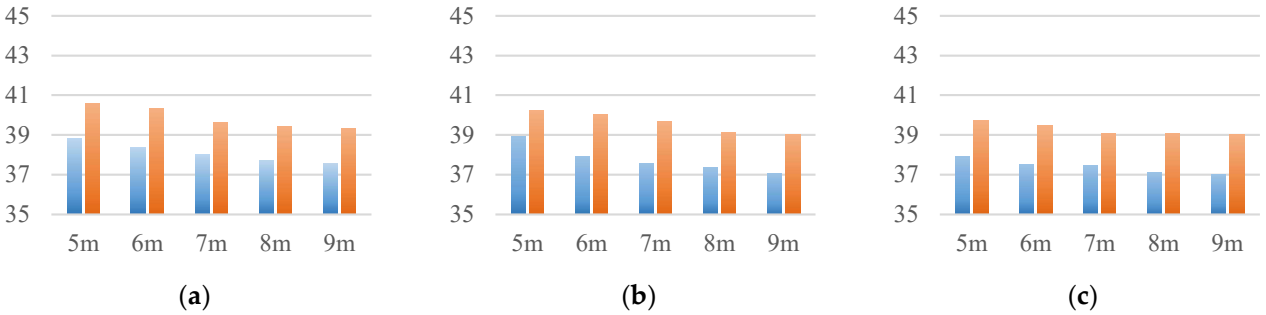

Figure 16. Average temperature in the whole greenhouse and crop zone according to the eave height of greenhouse (*X*-axis: eave height of greenhouse; *Y*-axis: Air temperature (°C); ■ Air temperature of the crop zone, ■ Average air temperature of the greenhouse). (**a**) External wind speed 0.5 m · s^{-1}, (**b**) External wind speed 1.5 m · s^{-1}, (**c**) External wind speed 3.0 m · s^{-1}.

3.4. Evaluation of the Ventilation Efficiency of the Improved Korean Venlo-Type Greenhouse with Continuous Roof Vents

The height difference between the upper and lower parts of the CR-Venlo greenhouse is sufficient due to the high eaves, and the buoyancy effect in hot summer is expected

to be particularly large due to the temperature differences between the upper and lower parts of the greenhouse. However, because the inflow and outflow of air occur through the same roof vent, they move against each other, resulting in the decreased efficiency of the greenhouse's inflow of external air and outflow of internal air.

In the CR-Venlo greenhouse, most of the inflow air from the roof vent on the windward side escapes through the opposite roof vent on the leeward side; therefore, the actual ventilation efficiency inside the greenhouse is considerably low. This phenomenon intensifies with an increase in airflow speed and is especially noticeable when ventilation based on external wind conditions is the dominant factor. Consequently, for wind ventilation, we designed and analyzed an improvement plan that involves changing the method of opening and closing the roof vents or opening the roof vent at a high angle, as well as installing a virtual windbreak to induce air inflow into the greenhouse.

In the models for Cases 1 and 2, which improved the operation of the opening and closing of the roof vents, the air inflow ($Air_{incoming}$) increased by 43% and 68%, respectively, compared to that in the existing model. In Case 3, the air inflow decreased by 35.6%. In Cases 1 and 2, the air inflow ($Air_{incoming}$) in the first span on the windward side increased markedly; a lot of air entered to the greenhouse in the central span where the separated air on the sidewall on the windward side entered the greenhouse. In Case 3, air inflow slightly increased in the leeward side span compared to that in the existing model; however, the air inflow ($Air_{incoming}$) decreased in most other spans.

The roof vent on the windward side was closed, and only the roof vent on the leeward side was open in Case 3; therefore, the air separated from the roof vent on the windward side entered through the roof vent on the leeward side. This model had significantly little air inflow ($Air_{incoming}$) in the span on the windward side, the central span, and the spans on the leeward side. In Case 3, the air separated at the roof vent on the windward side did not efficiently enter through the roof vent on the leeward side due to the short distance between the roof vents (Figure 17).

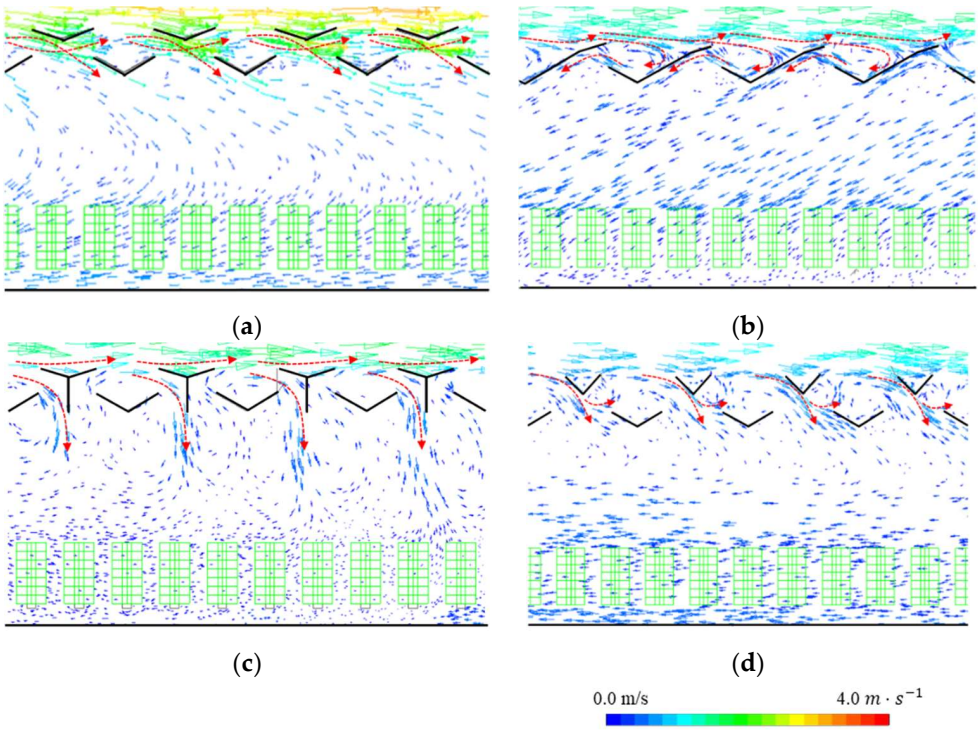

Figure 17. Airflow field from the roof windows of improved models: (**a**) Case 0: Korean multi-span greenhouse, (**b**) Case 3: Opening of all windward roof vents, (**c**) Case 4: Windbreak installation in the center of all roof vents, (**d**) Case 5: Increasing opening angle of roof vents.

In Case 4, where a virtual wall was installed on the roof vent of the CR-Venlo greenhouse, the amount of air inflow ($Air_{incoming}$) increased by approximately 43% compared to that in the existing model. Air inflow ($Air_{incoming}$) in the first span on the windward side increased markedly (0.89 kg·s^{-1} → 20.87 kg·s^{-1}). In Case 5, the amount of air inflow ($Air_{incoming}$) increased by approximately 95.9% compared to that in the existing model. Air inflow (Air_{inflow}) in the first span on the windward side increased markedly; the improvement was the greatest in the spans after the central span. The flow of air was induced toward the floor of the greenhouse due to the windbreak and the roof vent with a high opening angle (Figure 18). The structure directs the external air entering the greenhouse through the roof vent to the inside of the greenhouse. Therefore, a structure that effectively directs the external air entering through the roof vent to the inside of the greenhouse is important; in particular, the high opening angle of the roof vent is effective.

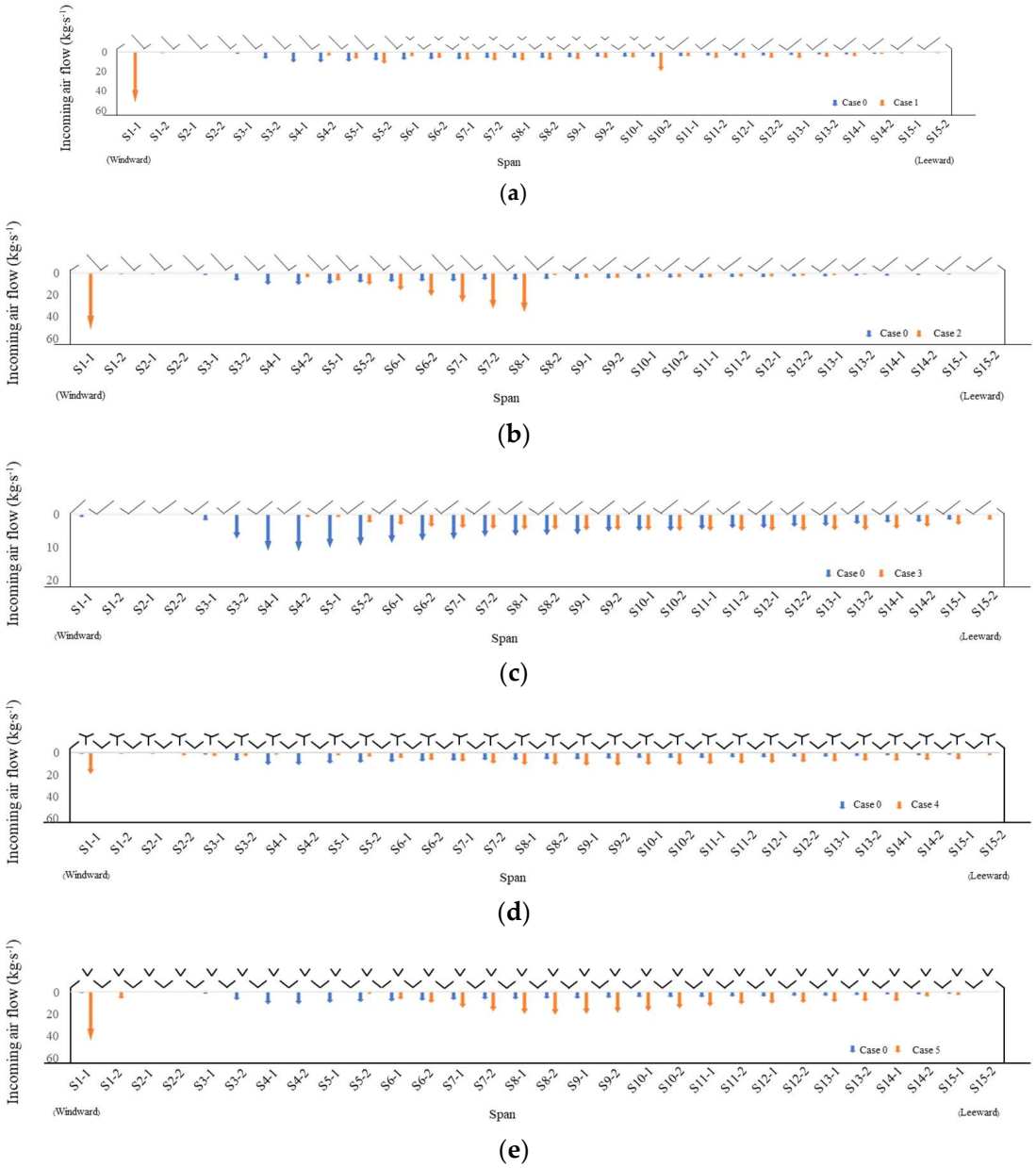

Figure 18. The incoming flow rate of the improved Korean Venlo-type greenhouse with continuous roof vents at an external wind speed of 3.0 m · s^{-1}. (**a**) Case 1, (**b**) Case 2, (**c**) Case 3, (**d**) Case 4, (**e**) Case 5.

Accordingly, the CR-Venlo greenhouse can replace a lot of air due to its large roof vent area; however, the considerably short distance between the roof vents and the open roof vents can cause a low ventilation rate; most of the air that enters through the roof vent escapes through the roof vent on the opposite side. The improvement plans in this study indicate that ventilation efficiency must be improved by managing the opening and closing of roof vents and installing walls.

4. Conclusions

This study evaluated the ventilation efficiency of a CR-Venlo greenhouse using CFD. Depending on wind speed, gravity with buoyancy driven ventilation and wind-driven ventilation were the dominant factors considering the air flow pattern in greenhouse and inflow/outflow rate. For an external wind speed of 0.5 $m \cdot s^{-1}$, gravity with buoyancy driven ventilation was the dominant factor, whereas the dominant factor was wind-driven ventilation, when the external wind speed was relatively fast at 1.5 and 3.0 $m \cdot s^{-1}$. In particular, when external wind ventilation was dominant, the air inflow (Air_{inflow}) through the roof vent was high, but the actual airflow rate into the greenhouse ($Air_{incoming}$) was significantly low, less than 30% in most cases.

The average greenhouse temperature and the average crop-zone temperature at varying heights of the CR-Venlo greenhouse revealed that, at a higher greenhouse height, the average temperatures of the greenhouse and crop zone decreased lognormally; this is consistent with the results of an earlier report [3]. Considering the exponential decrease in temperature with the increase in the height of the greenhouse, a height of 6 m or 7 m is efficient. However, the cost of greenhouse construction and maintenance should be considered.

In a CR-Venlo greenhouse, a lot of air flows in and out through the roof vent due to its wide structure; however, the amount of air entering the greenhouse was considerably low. Consequently, this study attempted to improve ventilation efficiency by managing the opening and closing of the greenhouse roof vent according to airflow. Based on the opening and closing of the roof vent, the air inflow rate ($Air_{incoming}$) inside the greenhouse either increased by 43 to 95.9% or decreased by 35.6%. Therefore, improving the ventilation rate for the CR-Venlo greenhouse requires a thorough evaluation of various conditions of the wind environment, conditions of opening and closing of the vent, and improvement plans for the roof vent. It may be that a controller may adjust vent opening according to wind speed and direction and thus improve ventilation efficiency.

Author Contributions: Conceptualization, S.-J.P. and I.-B.L.; methodology, S.-J.P.; S.-Y.L.; validation, S.-J.P. and H.-H.J.; investigation, S.-J.P., J.-G.K.; writing—original draft preparation, S.-J.P. and I.-B.L.; writing—review and editing, S.-J.P., C.D.-V., J.-H.C. and U.-H.Y.; visualization, Y.-B.C.; All authors have read and agreed to the published version of the manuscript.

Funding: This work was supported by the Korea Institute of Energy Technology Evaluation and Planning (KETEP) and the Ministry of Trade, Industry & Energy(MOTIE) of the Republic of Korea (No. 20212020800050).

Institutional Review Board Statement: Not applicable.

Informed Consent Statement: Not applicable.

Data Availability Statement: Not applicable.

Conflicts of Interest: The authors declare no conflict of interest.

References

1. Ministry of Agriculture Food and Rural Affairs. 2020. Available online: https://www.mafra.go.kr (accessed on 10 June 2022).
2. Flores-Velazquez, J.; Montero, J.I.; Baeza, E.J.; Lopez, J.C. Mechanical and natural ventilation systems in a greenhouse designed using computational fluid dynamics. *Int. J. Agric. Biol. Eng.* **2014**, *7*, 1.

3. Fatnassi, H.; Boulard, T.; Benamara, H.; Roy, J.C.; Suay, R.; Poncet, C. Increasing the height and multiplying the number of spans of greenhouse: How far can we go? In Proceedings of the International Symposium on New Technologies and Management for Greenhouses, Evora, Portugal, 19–23 July 2015; pp. 19–23.
4. Boulard, T.; Meneses, J.F.; Mermier, M.; Papadakis, G. The mechanisms involved in the natural ventilation of greenhouses. *Agric. Forest Meteorol.* **1996**, *79*, 61–77. [CrossRef]
5. Okushima, L.; Sase, S.; Lee, I.-B.; Bailey, B.J. Thermal environment and stress of workers in naturally ventilated greenhouses under mild climate. *Acta Hortic.* **2001**, *559*, 793–798. [CrossRef]
6. Bartzanas, T.; Boulard, T.; Kittas, C. Effect of vent arrangement on windward ventilation of a tunnel greenhouse. *Biosyst. Eng.* **2004**, *88*, 479–490. [CrossRef]
7. Kacira, M.; Sase, S.; Okushima, L. Effects of side vents and span numbers on wind-induced natural ventilation of a gothic multi-span greenhouse. *Jpn. Agric. Res. Q.* **2004**, *38*, 227–233. [CrossRef]
8. Baeza, E.J.; Pérez-Parra, J.J.; Montero, J.I.; Bailey, B.J.L.; Gázquez, J.C. Analysis of the role of sidewall vents on buoyancy-driven natural ventilation in parral-type greenhouses with and without insect screens using computational fluid dynamics. *Biosyst. Eng.* **2009**, *104*, 86–96. [CrossRef]
9. Fidaros, D.K.; Baxevanou, C.A.; Bartzanas, T.; Kittas, C. Numerical simulation of thermal behavior of a ventilated arc greenhouse during a solar day. *Renew. Energy* **2010**, *35*, 1380–1386. [CrossRef]
10. Ishii, M.; Okushima, L.; Moriyama, H.; Sase, S.; Fukuchi, N.; Both, A.J. Experimental study of natural ventilation in an open-roof greenhouse during the summer. In *ISHS Acta Horticulturae 1107: XXIX International Horticultural Congress on Horticulture: Sustaining Lives, Livelihoods and Landscapes (IHC2014): International Symposium on Innovation and New Technologies in Protected Cropping*; ISNS: Leuven, Belgium, 2014; pp. 67–74.
11. Ha, J. Evaluation of Natural Ventilation Efficiency of Protected Cultivation System in Reclaimed Land Using Aerodynamic Simulation. Master's Thesis, Seoul National University, Seoul, Korea, 2015.
12. Benni, S.; Tassinari, P.; Bonora, F.; Barbaresi, A.; Torreggiani, D. Efficacy of greenhouse natural ventilation: Environmental monitoring and cfd simulations of a study case. *Energy Build.* **2016**, *125*, 276–286. [CrossRef]
13. Boulard, T.; Roy, J.; Pouillard, J.; Fatnassi, H.; Grisey, A. Modelling of micrometeorology, canopy transpiration and photosynthesis in a closed greenhouse using computational fluid dynamics. *Biosyst. Eng.* **2017**, *158*, 110–133. [CrossRef]
14. Lee, S.Y.; Lee, I.B.; Kim, R.W. Evaluation of wind-driven natural ventilation of single-span greenhouses built on reclaimed coastal land. *Biosyst. Eng.* **2018**, *171*, 120–142. [CrossRef]
15. Zhao, Y.; Teitel, M.; Barak, M. Vertical temperature and humidity gradients in a naturally ventilated greenhouse. *J. Agric. Eng. Res.* **2001**, *78*, 431–436. [CrossRef]
16. Jung, D.H.; Kim, H.J.; Kim, J.Y.; Lee, T.S.; Park, S.H. Model predictive control via output feedback neural network for improved multi-window greenhouse ventilation control. *Sensors* **2020**, *20*, 1756. [CrossRef]
17. Chauhan, K.K.; Lunagaria, M.M. Interpolation of Microclimatic Parameters over Capsicum under Open Ventilated Greenhouse. *Int. J. Econ. Plants* **2022**, *9*, 95–100. [CrossRef]
18. Yeo, U.H.; Lee, S.Y.; Park, S.J.; Kim, J.G.; Choi, Y.B.; Kim, R.W.; Lee, I.B. Rooftop Greenhouse:(1) Design and Validation of a BES Model for a Plastic-Covered Greenhouse Considering the Tomato Crop Model and Natural Ventilation Characteristics. *Agriculture* **2022**, *12*, 903. [CrossRef]
19. Chung, S.J.; Seo, B.S.; Kang, J.K.; Kim, H.G. Development of hydroponic technique of fruit vegetables using perlite and mixtures with perlite as a substrate: 1. Effects of containers and substrates on the growth and fruit quality of hydroponically grown cucumber. *J. Bio-Environ. Control.* **1995**, *4*, 159–166.
20. Kim, R.W.; Lee, I.B.; Yeo, U.H.; Lee, S.Y. Evaluation of various national greenhouse design standards for wind loading. *Biosyst. Eng.* **2019**, *188*, 136–154. [CrossRef]
21. Norton, T.; Grant, J.; Fallon, R.; Sun, D.-W. Improving the representation of thermal boundary conditions of livestock during CFD modelling of the indoor environment. *Comput. Electron.* **2010**, *73*, 17–36. [CrossRef]
22. Seo, I.-H.; Lee, I.-B.; Moon, O.-K.; Hong, S.-W.; Hwang, H.-S.; Bitog, J.P.; Kwon, K.; Ye, Z.; Lee, J. Modelling of internal environmental conditions in a full-scale commercial pig house containing animals. *Biosyst. Eng.* **2012**, *111*, 91–106. [CrossRef]
23. Wu, W.; Zhai, J.; Zhang, G.; Nielsen, P.V. Evaluation of methods for determining air exchange rate in a naturally ventilated dairy cattle building with large openings using computational fluid dynamics (CFD). *Atmos. Environ.* **2012**, *63*, 179–188. [CrossRef]
24. Yeo, U.H.; Lee, I.B.; Kim, R.W.; Lee, S.Y.; Kim, J.G. Computational fluid dynamics evaluation of pig house ventilation systems for improving the internal rearing environment. *Biosyst. Eng.* **2019**, *186*, 259–278. [CrossRef]
25. Lee, M.H. Analysis of Aerodynamic Improvements about Major Environmental Problems in Highrise Multi-Span Greenhouse. Master's Thesis, Seoul National University, Seoul, Korea, 2019.
26. Richards, P. *Computational Modelling of Wind Flow Around Low-Rise Buildings Using PHOENICS*; AFRC Institute of Engineering Research: Silsoe, UK, 1989.
27. Bartzanas, T.; Kittas, C.; Sapounas, A.; Nikita-Martzopoulou, C. Analysis of airflow through experimental rural buildings: Sensitivity to turbulence models. *Biosyst. Eng.* **2007**, *97*, 229–239. [CrossRef]
28. Bournet, P.E.; Ould Khaoua, S.A.; Boulard, T. Numerical prediction of the effect of vent arrangements on the ventilation and energy transfer in a multi-span glasshouse using a bi-band radiation model. *Biosyst. Eng.* **2007**, *98*, 224–234. [CrossRef]

29. Bournet, P.-E.; Boulard, T. Effect of ventilator configuration on the distributed climate of greenhouses: A review of experimental and CFD studies. *Comput. Electron. Agric.* **2010**, *74*, 195–217. [CrossRef]
30. Tominaga, Y.; Mochida, A.; Murakami, S.; Sawaki, S. Comparison of various revised Ke 3 models and les applied to flow around a high-rise building model with 1:1:2 shape placed within the surface boundary layer. *J. Wind Eng. Ind. Aerodyn.* **2008**, *96*, 389–411. [CrossRef]
31. Kim, R.W.; Lee, I.B.; Kwon, K.S. Evaluation of wind pressure acting on multi-span greenhouses using CFD technique, part 1: Development of the CFD model. *Biosyst. Eng.* **2017**, *164*, 235–256. [CrossRef]
32. Papadakis, G.; Mermier, M.; Meneses, J.F.; Boulard, T. Measurement and analysis of air exchange rates in a greenhouse with continuous roof and side openings. *J. Agric. Eng. Res.* **1996**, *63*, 219–227. [CrossRef]